International Journal of
Science and Engineering Investigations vol. 1, issue 8, September 2012
ISSN: 2251-8843

Predictions of NOx and Soot Emissions in Converging and Diverging Ducts

Mohammad Moghiman[1], Maryam Amiri[2], Amirhosein Amiri[3]
[1,2]Faculty of mechanical Engineering, Ferdowsi University of Mashhad, Iran
[3]Faculty of Chemical and Petroleum Engineering, Sharif University of Technology, Iran
([1]moghiman@yahoo.com, [2] maryamamiri272@gmail.com, [3]amiri@che.sharif.ir)

Abstract- The influences of air preheating and diverging angle on combustion characteristics, NOx and Soot emission in the converging and diverging ducts are studied with numerical simulation. The differential equations in the Von Misses coordinate system are transformed to a cross-stream coordinate system to be able to concentrate more grid lines near wall boundaries. A marching integration solution procedure employing the TDMA is used to solve the discretized equations. In this system, by the use of a general variable, the mass, momentum, energy, and chemical species conservation equations have been written in a total form. The nature of the governing differential equation is parabolic. Also, the considered flow in this research is an incompressible flow with a compressible fluid, which its Mach numbers are less than 0.3 and it has high Peclet number. The flow behavior in the vicinity of the walls is measured through utilizing the wall function method. The considered turbulence model is the Prandtl Mixing Length method. Modeling the combustion process, in other words, measuring the amount of fuel consumption and the energy released as a result of combustion process is done by the use of Arrhenius and Eddy Dissipation method. Thermal mechanism has been utilized for modeling the process of forming the nitrogen oxides. Khan and Greeves model is used for modeling the process of Soot formation. Finite difference method and Genmix numerical code are used for numerical solution of equations. Our results indicate the important influence of the limiting diverging angle of diffuser on the coefficient of recovering of pressure. By air preheating, emission of pollutants increased. Also, the converging and diverging effect of duct on its output behavior have been indicated.

Keywords- *Air preheating; Combustion; Converging and Diverging Duct; Diverging Angle ; NOx; Soot.*

I. INTRODUCTION

The necessity to decrease of velocity and preventing the pressure loss in most of the inside flow lead to the use of diffuser in various kinds [1]. In gas turbine, which is actually a thermal motor, and in which the air is used as the operating fluid for creating pressure, diffusers play a main role in converting the kinetic energy into pressure energy. Aerodynamic of diffusers also play important role in controlling the distribution of the mass flow, the stability of the combustion chamber system, and decreasing of the pressure loss of the turbine gas [2]. The air entering into the airplane engines is provided through channel to the form of the diffuser having the Mach number range number of 0.4 and the less, which in flight condition the high Mach number lead to increasing the pressure [3]. In these engines, the effect of low pressure drop and the uniformity of the flow to prevent of vibration are of great importance.

In flow of boundary layer inside the diffuser having flat walls, diverging angle has considerable importance. If this angle is very small, the length of diffuser will become long and the friction losses will increase and too much enlarging of this angle leads to separation of boundary layer and production of recirculation and consequently the losses of fluid power [4,5].

The flow with proper diverging angle is a kind of boundary layer and the equations can be solved through using marching method. This method has significant advantages over other calculating methods with a view to the speed of doing calculations and also the memory volume for doing calculations [5,6]. In numerical simulations, the flow being inside the diffusers and also the grid conformity to solution zone and increasing its compression in the vicinity of the solid wall play a great role in accuracy of the gained results [7]. One of the approaches utilized for gaining the conformity of calculating grid to solution field , is the use of Von Misses coordinate, in which flow lines are chose as one of the independent coordinates [8]. Sadakata and Fujioka and Kunii [9] investigated the effects of air preheating on the emission of NO, HCN and NH3 from an ordinary single-stage combustion and a two-stage combustion, with the hope of finding an ideal combustion method which can realize both energy savings and NOx reduction. Wang and Cai and Xie [10] studied the effect of air preheating temperature, oxygen concentration, and fuel inlet temperature on flame properties, and NOx formation and emission in the furnace.

The purpose of this paper is development of a numerical method to measure the parabolic flow inside and outside the converging and diverging ducts in combustive situation and numerical simulation of the NOx and Soot pollutants. The effects of the important parameters such as limiting diverging

angle and air preheating on NOx and Soot emissions are also studied.

II. GOVERNING EQUATIONS AND SELECTION THE COORDINATES SYSTEM

Momentum (1), energy (2), and chemical species conservation (3) equations in coordinates set is on the basis of stream lines x~ψ [8] as follows:

$$\frac{\partial U}{\partial x} = \frac{\partial}{\partial \psi}\left(r^2 \rho U \mu_{eff} \frac{\partial U}{\partial \psi}\right) + \frac{1}{\rho U}\left(F_x - \frac{\partial P}{\partial x}\right) \quad (1)$$

$$\frac{\partial \tilde{h}}{\partial x} = \frac{\partial}{\partial \psi}\left(\frac{\partial}{\partial \psi}\left(r^2 \rho U \Gamma_{h,eff} \frac{\partial \tilde{h}}{\partial \psi}\right)\right) + \frac{\partial}{\partial \psi}\left[\left(\mu_{eff} - \Gamma_{h,eff}\right) r^2 \rho U \frac{\partial\left(U^2/2\right)}{\partial \psi}\right] \quad (2)$$

$$\frac{\partial m_j}{\partial x} = \frac{\partial}{\partial \psi}\left(r^2 \rho U \Gamma_{j,eff} \frac{\partial m_j}{\partial \psi}\right) + \frac{R_j}{\rho U} \quad (3)$$

$$\frac{\partial (m_{ox} - m_{fu} s)}{\partial x} = \frac{\partial}{\partial \psi}\left(r^2 \rho U \Gamma_{eff} \frac{\partial (m_{ox} - m_{fu} s)}{\partial \psi}\right) \quad (4)$$

It should be noted that one of the independent variables of the coordinates set is stream function (ψ) that considering its definition and satisfying the continuity equation, there is no need to solve the continuity equation. In above equation the dependent variables $(m_{ox} - m_{fu}s), m_j, \tilde{h}$, U are indicated with the general variable ∅ and through changing the variable $\omega = \frac{\psi - \psi_E}{\psi_E - \psi_I}$ instead of ψ the above differential equations can be written in a total form as follows:

$$\frac{\partial \emptyset}{\partial x} + (a + b\omega)\frac{\partial \emptyset}{\partial \omega} = \frac{\partial}{\partial \omega}\left(c \frac{\partial \emptyset}{\partial \omega}\right) + d \quad (5)$$

Coefficients as following; a, b, c, d:

$$a = \frac{r_I \dot{m}''_I}{(\psi_E - \psi_I)} \quad b = \frac{(r_E \dot{m}''_E - r_I \dot{m}''_I)}{(\psi_E - \psi_I)} \quad c = \frac{r^2 \rho U \Gamma_{eff}}{(\psi_E - \psi_I)^2} \quad d = \frac{1}{\rho U} S_\emptyset \quad (6)$$

In above relation $S_\emptyset$ source term for the variable ∅ ,$\dot{m}''_I$,$\dot{m}''_E$the rate of mass flow from the boundaries I ,E and also ψ_I,$\psi_E$the amount of the stream function are boundaries I, E. Turbulence effects has been measured by the use Prandtl mixing length method.to measure the features of the flow in the vicinity of the solid boundaries, The wall function provided by the help of the theory of the Couette flow have been utilized [11]:

$$y^+ < 11.63 \qquad y^+ = U^+ \quad (7)$$

$$y^+ > 11.63 \qquad U^+ = \frac{1}{K}\left[2\left((1 + P^+ y^+)^{1/2} - 1\right) + \ln\left(\frac{4Ey^+}{2 + P^+ y^+ + 2(1 + P^+ y^+)^{1/2}}\right)\right] \quad (8)$$

$$\tilde{h}^+ = \sigma_t (U^+ + P_h) + (1 - \sigma_t) W \frac{(U^+)^2}{2} \quad (9)$$

$$m_j^+ = \sigma_t \left(U^+ + P_j\right) \quad (10)$$

The sign (+) is indicators of the dimensions less in parameters, and the values of K and E are constants which all the turbulent flows crossing on the flat wall are $K = 0.4, E = 9.8$ .The values P_h and $P_j$are dependent upon the Prandtl-Schmidt number of laminar to Prandtl-Schmidt number of turbulence ratio.

$$P = 9.24\left[\left(\frac{\sigma_l}{\sigma_t}\right)^{0.75} - 1\right]\left(1 + 0.28 \exp\left[-0.007\left(\frac{\sigma_l}{\sigma_t}\right)\right]\right) \quad (11)$$

The energy due to combustion is determined in consideration of a single step, irreversible, global reaction between the fuel vapor and oxygen. The reaction rates that appear as source terms in species transport equations are computed by using the eddy dissipation method (12) [12] and Arrhenius rate (13) [13]. The rate of fuel consumption is measured by two calculating methods and the smallest of them with consideration of the effects of mixing is selected.

$$R_{fu} = -C\, \rho\, m_{fu} \left|\frac{\partial U}{\partial y}\right| \quad (12)$$

$$R_{fu} = -p P^2 m_{fu} m_{ox} \exp\left\{-\frac{E}{RT}\right\} \quad (13)$$

III. POLLUTANTS FORMATION MODELS

Pollution arising from the nitrogen oxides has prejudicial effects on the health of human beings and the environment, and it also plays a great role on the forming the acid rains, fog, chemical smoke and perforation of the ozone layer. The annual production of these gasses has been raised six times since 1950.

The collection of the NO and NO2 is called NOx that is formed through combustion processes and the chemical reaction of nitrogen present in combustion air and/or in-fuel nitrogen. Chiefly, for production of NOx in combustion of gas fuels, three mechanisms are brought into forth:

Thermal mechanism [14], prompt mechanism [14,15], and fuel mechanism [14].

The thermal NOx formation mechanism proposed by Zeldovich [12], accounts for the oxidation of the nitrogen. The formation thermal NOx is highly dependent on the peak flame temperature and oxygen availability. Once oxygen atoms are formed, then oxidation of atmospheric nitrogen via the thermal NO (Zeldovich) mechanism takes place as follows:

$$O + N_2 \rightleftarrows NO + N \quad (14)$$

$$N + O_2 \rightleftarrows NO + O \quad (15)$$

The first reaction is generally rate controlling, since breaking the N_2bond is most difficult step in the Zeldovich mechanism. Both reactions are very important in terms of NO formation. In addition, another reaction has been proposed by Lavoie and Heywood and Keck [16]:

$$N + OH \leftrightarrow NO + H \quad (16)$$

This reaction is important in fuel-rich flames and can be ignored in most fuel lean NO calculations [17]. In this study, the rate constants for forward and reverse reactions (14) and (15) are selected from the work of Hanson and Salimian [18]:

$$R_{f1} = 1.8 * 10^8 * EXP\left(\frac{-38370}{T}\right) \quad (17)$$

$$R_{f2} = 1.8 * 10^4 * T * EXP\left(\frac{-4680}{T}\right) \quad (18)$$

$$R_{r1} = 3.8 * 10^7 * EXP\left(\frac{-425}{T}\right) \quad (19)$$

$$R_{r2} = 3.8 * 10^3 * T * EXP\left(\frac{-20820}{T}\right) \quad (20)$$

The NO formation rate via thermal NO mechanism is given as [15]:

$$\frac{d[NO]}{dt} = \frac{2[O]\{R_{f1}R_{f2}[O_2][N_2] - R_{r1}R_{r2}[NO]^2\}}{R_{f2}[O_2] + R_{r1}[NO]} \quad (21)$$

At equilibrium, the rate of formation of NO is zero and the concentration of NO is found from the following equation:

$$\frac{2[O]\{R_{f1}R_{f2}[O_2][N_2] - R_{r1}R_{r2}[NO]^2\}}{R_{f2}[O_2] + R_{r1}[NO]} = 0 \quad (22)$$

The concentration of O_2 and N_2 are calculated in the combustion solution and $[O]$ radical concentration can be determined by the partial equilibrium assumption [19]:

$$[O] = 36.64 * T^{1/2} * [O_2]^{1/2} EXP\left(\frac{-27123}{T}\right) \quad (23)$$

Fuel NO is formed through oxidation of nitrogenous composites of the fuel in flame part, and when the amount of the fuel Nitrogen is more than the one-tenth (0.1) of the fuel weight, its production is considerable. The prompt NOx mechanism which first was reported by Fenimor describes the reaction of the atmospheric nitrogen with hydrocarbon fuel fragments before either undergoing oxidation to NO or reduction to N_2. The prompt NOx formation is most prominent in fuel rich regions where an abundance of hydrocarbon fragments are available. In order to predict the amount of the NO in this research, the Zeldovich Model is used which it measures successfully the NO concentration. Considering that in this model relatively small amount of computer memory is necessary, so it is economical and this fact is an important factor in selecting the model for NO modeling.

The Khan and Greeves model and Magnussen combustion model are used for modeling the processes of Soot formation and combustion. This model is empirically -based [15]. R_{soot} , the net rate of soot generation, is the balance of soot formation, $R_{soot,form}$, and soot combustion, $R_{soot,comb}$:

$$R_{soot} = R_{soot,form} - R_{soot,comb} \quad (24)$$

The rate of soot combustion is the minimum of two rate expression:

$$R_{soot,form} = C_s P_{fuel} \emptyset^r e^{-E/RT} \quad (25)$$

Where C_s is the soot formation constant and P_{fuel} , fuel partial pressure and $\emptyset$, equivalence ratio, and r equivalence ratio exponent and E/R ,activation temperature, according to [15]. The rate of soot combustion is the minimum of two rate expressions:

$$R_{soot,comb} = min[R_1, R_2] \quad (26)$$

The two rates are computed as:

$$R_1 = A\,\rho\, m_{soot}\,\frac{\varepsilon}{K} \quad (27)$$

And

$$R_2 = A\,\rho\,\left(\frac{m_{ox}}{\upsilon_{soot}}\right)\left(\frac{m_{soot}\,\upsilon_{soot}}{m_{soot}\,\upsilon_{soot} + m_{fu}\,\upsilon_{fu}}\right)\frac{\varepsilon}{K} \quad (28)$$

Where A is the constant in the Magnussen model, and m_{ox} , m_{fu} , mass fractions of oxidizer and fuel, and υ_{soot} , υ_{fu} mass stoichiometries for soot and fuel combustion.

IV. GRID GENERATION AND SOLVING THE DIFFERENTIAL EQUATION

Grid generation in the field of calculation is done through consideration of the coordinates x and ω. Considering the parabolic nature of the total equation 5 it can be solved by the use of the marching method [20] along the flow. In this method, it is supposed that each node in the grid is influenced at the most by the 5 upstream nodes and neighbor nodes, which two points in its neighbor and three points in its upstream section are placed.

$$D_i\emptyset_{i,D} = A_i\emptyset_{i+1,D} + B_i\emptyset_{i-1,D} + E_i\emptyset_{i,U} + F_i\emptyset_{i+1,U} + G_i\emptyset_{i-1,U} + H_i \quad (29)$$

The index U and Dare indicators of the upstream and downstream section of the flow which the upstream values are active and the downstream values are passive. Therefore, all the active values can be placed inc_i .

$$D_i\emptyset_{i,D} - A_i\emptyset_{i+1,D} - B_i\emptyset_{i-1,D} = C_i \quad (30)$$

The coefficientsA_i,B_i...also is produced through integration of the conservation equation on the computational element.

$$A_i = \left(T - \frac{1}{2}\dot{m}'\right)_{i+\frac{1}{2}} \quad (31)$$

$$B_i = \left(T + \frac{1}{2}\dot{m}'\right)_{i-\frac{1}{2}} \quad (32)$$

$$C_i = \emptyset_{i,D} P\left(\omega_{i+\frac{1}{2}} - \omega_{i-\frac{1}{2}}\right) + S_i \quad (33)$$

$$D_i = A_i + B_i + P\left(\omega_{i+\frac{1}{2}} - \omega_{i-\frac{1}{2}}\right) - S_i \quad (34)$$

Which in the above relations:

$$P = \frac{(\psi_E - \psi_I)_U}{\delta x} \qquad T_{i\pm\frac{1}{2}} = \frac{(r\Gamma_{eff})_{i\pm\frac{1}{2}}}{\pm(y_{i\pm1} - y_i)_U} \quad (35)$$

By expansion of the (30) for the passive points of the each section, we will reach to an equation system having the matrix of three-diameter coefficients. This equation system is solved by TDMA algorithm.

V. CALCULATION OF THE PRESSURE FIELD

In fluid flow inside the converging and diverging ducts, the pressure changes due to the change of flow section is considerable, is a great role in calculation of flow field. The cross section between the two lines of flows (1&2) can be written as follows [20]:

$$A_{12} = \int_1^2 \frac{d\psi}{\rho U} \quad (36)$$

Through differentiation of the above relation in proportion to pressure and the use of the relation between the speed of sound and fluid thermodynamic properties, it can be written:

$$\frac{dP}{dA_{12}} = \frac{1}{\int_1^2 \frac{1}{\rho^2 U^3}(1-M^2)d\psi} \quad (37)$$

In which M is the fluid mach number.

Through knowing the changes of the pressure in proportion to cross section and the determination of the geometry of flow field (the changes of the section level along the flow), the pressure changes on the path of the flow can be calculated.

$$\frac{dP}{dx} = \frac{\frac{dA_{12}}{dx}}{\int_1^2 \frac{1}{\rho^2 U^3}(1-M^2)d\psi} \quad (38)$$

VI. OPEARATING PARAMETERS AND BOUNDARY CONDITIONS

The considered flow in this research is an incompressible flow with a compressible fluid, which its Mach numbers are less than 0.3 and it has high Peclet number. Considering the parabolic nature of the flow, the boundary conditions are determined in three boundaries of the four boundaries, in other words in entrance section and the surrounding walls. The air and fuel vapor enter the duct with a temperature of 300K and 500k respectively and axial velocity of air is 30 m/s. The liquid fuel is considered to be kerosene ($C_{12}H_{23}$).

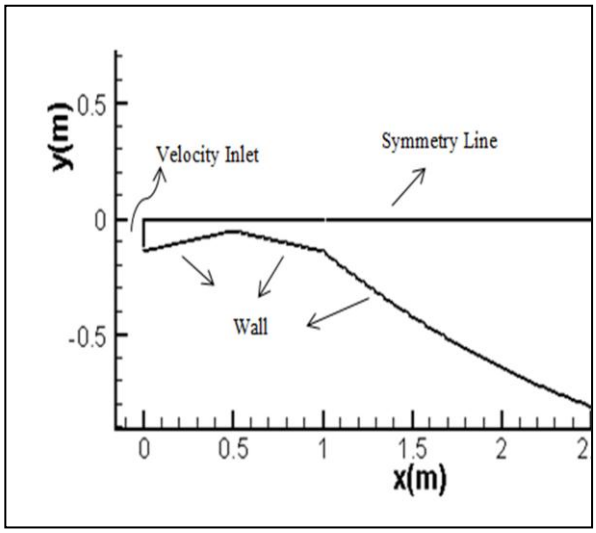

Figure1. Characteristic of duct and boundary condition

VII. NUMERICAL MESH

A numerical mesh of 61* 20 grid nodes is used after several experiments, which shows that further refinement in either direction does not changed the result by more than 2%. The grid spacing in axial and radial directions are changed smoothly to minimize the deterioration of the formal accuracy of the finite difference scheme due to variable grid spacing and in such a way that higher concentration of nodes occur near the inlet and the walls.

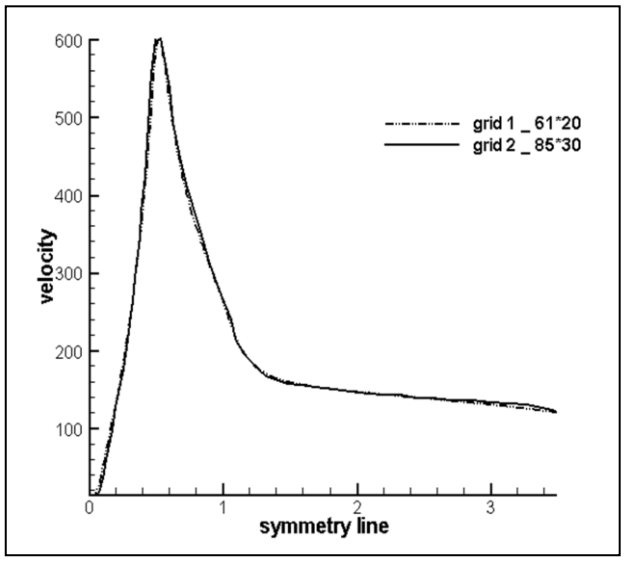

Figure2. The effect of grid size on the centerline velocity distribution

VIII. RESULTS

In Fig. 3 the numerical calculations results are compared with Fox and Kline experimental results [21] regarding the flat diffuser. In this figure, the effect of the length to diameter ratio of the input section upon the limiting angle of the diffuser head has been showed. The results of two numerical and experimental methods show satisfactory agreement (particularly, in the proportionalities of length to entrance diameter of more than 10). The consequences of these two approaches indicate that if the length proportionalities to entrance diameter decrease from about 10, limiting diverging angle (largest angle before fluid separation from wall) increase quickly.

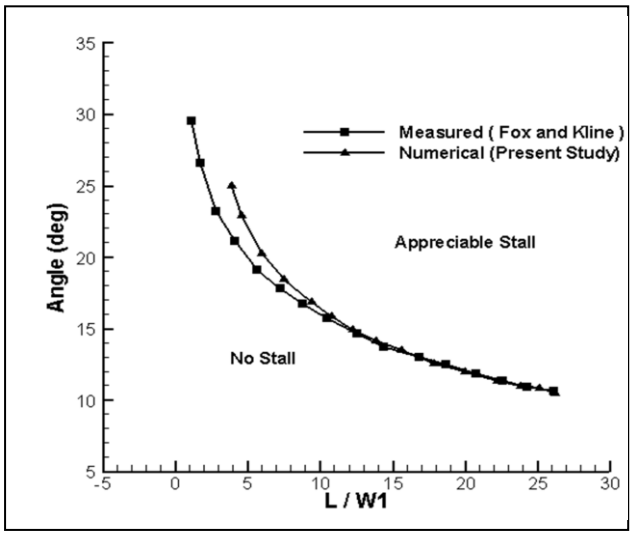

Figure3. Comparison of numerical calculations and experimental results for limiting diverging angles

Fig.4 presents the results of the pressure recovery coefficient (C_{PR}) defined as $C_{PR} = 1 - (U_2/U_1)^2$ ideally by using Fox and Kline [21] (as U_1 , U_2 are respectively the velocities of input and output sections). The results of the experimental measurements [21] and the results of the ideal conditions for the length to diameter ratio of the input equal to 10 have been compared. The ideal condition results and the numerical results are very close and a little more than the experimental results. The difference between the experimental results with two different methods can be due to not considering the effects of input and output sections and also the influence of the roughness of the diffuser experimental walls that it leads to wasting of energy. As a whole, these three methods have same changes process.

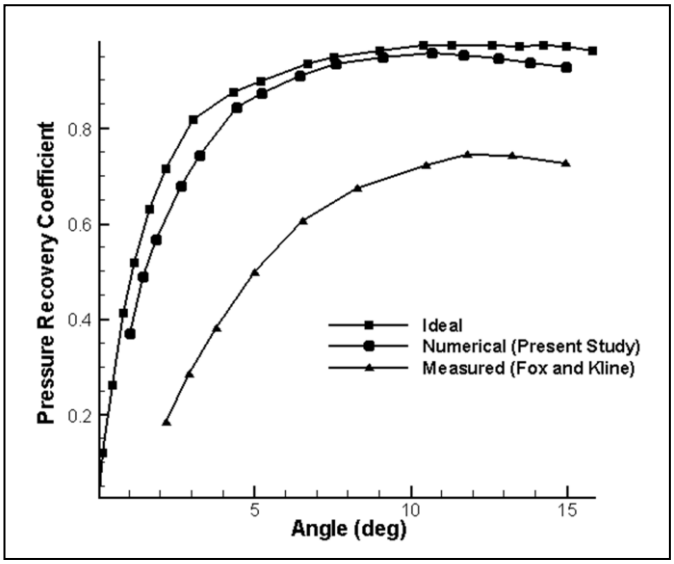

Figure4. Comparison of numerical calculations and experimental C_{PR} results for different diverging angles

In rockets and launch systems the propulsion force is driven by the thrust chamber which includes combustion chamber and diffuser. The effect of the variation of diverging angle on velocity in converging and diverging duct is shown in Fig. 5.The result show that increasing diverging angle led to increasing of velocity in the combustion chamber (converging) and reducing of velocity in the flat diffuser. Also with increasing of diverging angle, combustion rate will increase (Fig. 6).

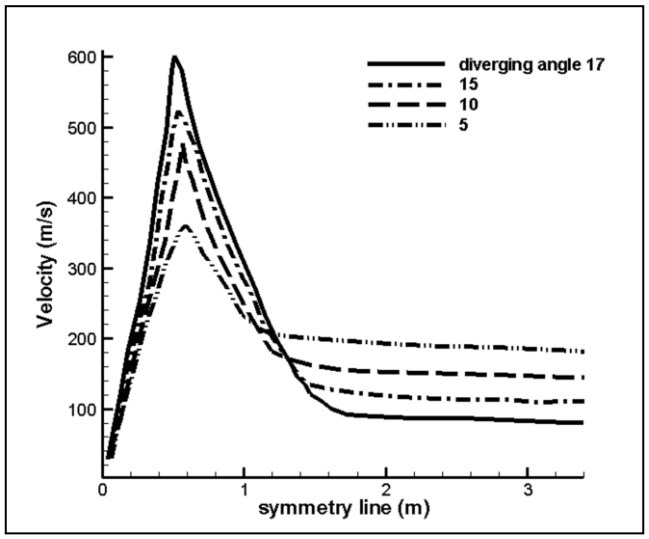

Figure5. The effect of the variation of diverging angle on velocity in converging and diverging duct

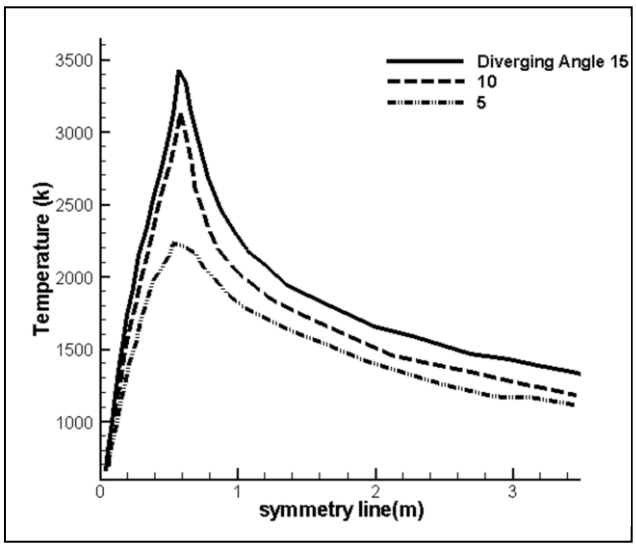

Figure6. The effect of the variation of diverging angle on temperature in converging and diverging duct

Due to the intense dependence of NOx pollutant to the maximum temperature, with increasing of combustion rate, mass fraction of NOx pollutant will increase (Fig. 7).

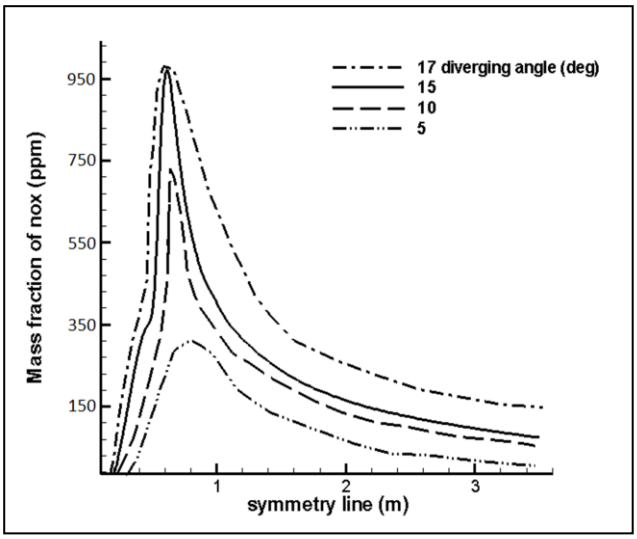

Figure7. The effect of the variation of diverging angle on mass fraction of NOx in converging and diverging duct

It is well known that recovering flue gas heat to pre-heat combustion air is one of the most practical and effective means of saving energy. However, as air preheating increases the flame temperature, it follows that air preheating has the undesirable effect of increasing emissions of NOx (Figs. 8&9).

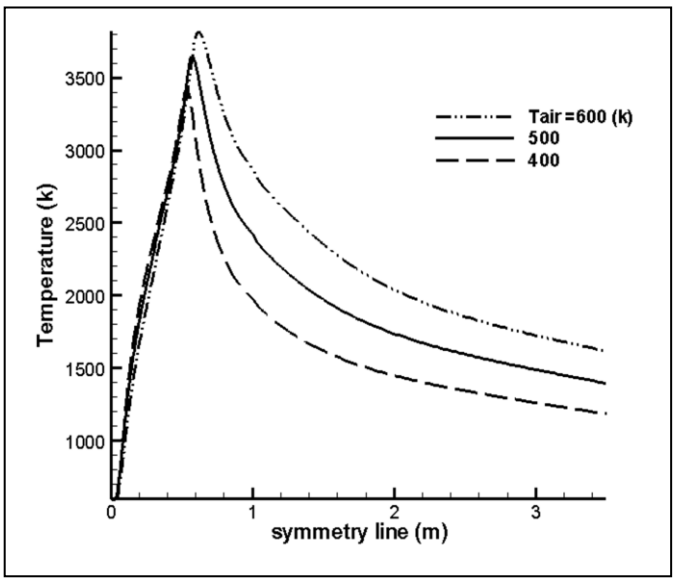

Figure8. The effect of the air preheating on temperature in converging and diverging duct

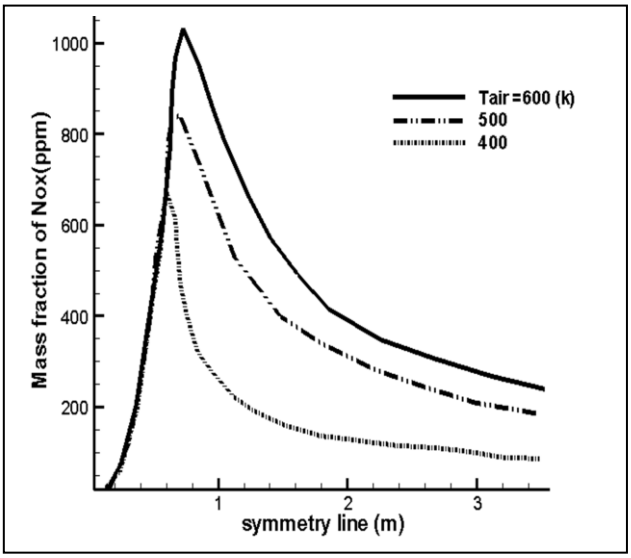

Figure9. The effect of the air preheating on mass fraction of NOx in converging and diverging duct

But increasing the air temperature has a complex effect on soot formation. The amount of soot formation in flame increases by air preheating. On the other hand, high flame temperature results in soot combustion and decreasing in output (Fig. 10).

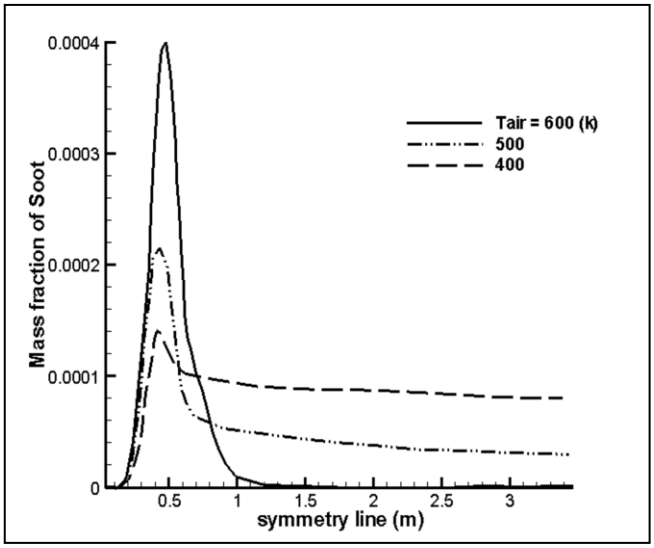

Figure10. The effect of the air preheating on mass fraction of Soot in converging and diverging duct

IX. CONCLUSIONS

In this paper, combustive incompressible parabolic flow has been simulated by the use of marching method inside and outside the converging and diverging ducts, and reports on the results of a numerical investigation on the effects of air preheating on NOx and Soot emissions in converging and diverging ducts. The converging and diverging effect of duct on its output behavior have been indicated. Due to the intense dependence of Nox pollutant to the maximum temperature in the domain with this feature, the Nox pollutant amount is also in maximum level. By preheating air for the combustion, emission of NOx and Soot increased. Using the marching method reduce considerably the time and the memory necessary for calculation.

ACKNOWLEDGMENT

The support of Ferdowsi University for funding of this study is gratefully acknowledged.

REFERENCES

[1] R. S .Azad, "Turbulent flow in conical diffuser," Experimental Thermal and Fluid Science, vol.13, 1996, pp.318-337.

[2] A. H. Lefebver, "Gas Turbine combustion, " Mc Graw-Hill, Newyork, 1983.

[3] P. G .Hill and C. R. Peterson, "Mechanic and thermodynamic of propulsion , "Addison-Wesley Company, Massachusetts, 1965.

[4] V. Ganesan, K. Suzuki, P .A. Narayana, and V. K .Chithambaran, "Investigations of mean and turbulent flow characteristics of a two dimensional plane diffuser , "Experiment in Fluids, vol.10,1991, pp.205-212.

[5] A. Olsson, G. Stemme and E .Stemme , "Numerical and experimental studies of flat-walled diffuser element for valve-Less micro pumps,"Sensors and Actuators A,2000, pp.165-175.

[6] G. Gan and S. B. Riffat, "Measurement and computational fluid dynamics prediction of pressure-loss coefficient, "Applied Energy,vol.54, 1996, pp.181-195.

[7] W. Sky, "A numerical study of dump diffuser flow, " Computer Method in Applied Mechanic and Engineering, vol.53,1985,pp. 47-65.

[8] C. A. J. Fletchers, "Computation techniques for fluid dynamics, "vol.2,1988.

[9] M. Sadakata, Y. Fujioka and D. Kunii, "Effects of preheating on emissions of NO, HCN and NH_3 from a two-stage combustion, "Eighteenth Symposium (International) on Combustion, 1981.

[10] A. Wang, J. Cai and G. Xie, "Numerical simulation of combustion characteristics in high temperature air combustion furnace, " Journal of Iron and Steel Research,vol.16, 2009, pp. 06-10.

[11] B. E. Launder and N. Shima, "Second-moment closure for the wall sub layer, development and application, " AIAA Journal,vol.27, 1989, pp.1319-1325.

[12] B. F. Magnussen, "Modeling of pollutant formation in gas turbine combustors based on the eddy dissipation concept, "18th International Congress on Combustion Engines, International Council on Combustion Engines, 1989.

[13] I. Glassman, "Combustion, " Academic Press, 1996.

[14] A. Beltrame, P. Porshnev, M. W. Merchan, A .Saveliev ,A. Fridman, L. A. Kennedy, O .Petrova, S .Zhdnok, F. Amouri and O .Charon, "Soot and NO formation in methane–oxygen fnriched diffusion flames, " Journal of Combustion and Flame, vol.124,2001, pp.295–310.

[15] FLUENT 6.3 User's Guide, Fluent Inc, 2006.

[16] G. A. Lavoie, j. B. Heywood, and, J.C. Keck, "Experimental and theoretical study of nitric oxide formation in internal combustion engines, " Combustion Science Technology, 1970.

[17] G. G. D. Soete, "Fundamental chemistry of NOx and N_2O formation and destruction, "Third flame research coarse, IFRF, The Netherlands, 1990.

[18] R. K. Hanson and S. Salimian, "Survey of rate constants in H/N/O system, " Combustion Chemistry, 1984.

[19] J. Warnatz, U. Mass, and R.W. Dibble, "Combustion, physical and chemical fundamentals, modeling and simulation, experiments, pollutant formation, "4th Edition, Springer ,2006.

[20] D.B. Spalding, "GENMIX-A general computer program for two-dimensional parabolic phenomena, "Pergamon New York, 1977.

[21] R. W. Fox, S. J .Kline, Flow regime data and design method for curved subsonic diffusers, ASME Journal of Basic Engineering, vol.84,1962, pp. 303-312.

NOMENCLATURE

A,B,C,D	Coefficient
E	Activation energy
$\tilde{h}$	Enthalpy
m	Mass fraction
$\dot{m}''_I$	Rate of mass flow from the boundaries I
$\dot{m}''_E$	Rate of mass flow from the boundaries E
P	Pressure
p	Constant
r	Radial direction
R_f , R_r	Rate constant for forward and reverse reaction
s	Stoichiometric coefficient
S	Source term
T	Temperature
U	Velocity
x	Axial direction

Greek symbols

σ_l , σ_t	Empirical coefficient
Γ	Diffusion coefficient
ψ	Stream function
μ	Dynamic viscosity
$\emptyset$	General variable
ω	Dimensionless Stream function
ρ	Density

Subscript

D	Downstream
U	Upstream